

3D printing of versatile reactionware for chemical synthesis

Philip J Kitson^{1,2}, Stefan Glatzel², Wei Chen³, Chang-Gen Lin¹, Yu-Fei Song^{1,3} & Leroy Cronin^{1,2}

¹International Research Centre for Soft Matter, Beijing University of Chemical Technology, Beijing, P. R. China. ²WestCHEM, School of Chemistry, The University of Glasgow, University Avenue, Glasgow, UK. ³State Key Laboratory of Chemical Resource Engineering, Beijing University of Chemical Technology, Beijing, P. R. China. Correspondence should be addressed to Y.-F.S. (songyf@mail.buct.edu.cn) or L.C. (Lee.Cronin@glasgow.ac.uk).

Published online 14 April 2016; doi:10.1038/nprot.2016.041

In recent decades, 3D printing (also known as additive manufacturing) techniques have moved beyond their traditional applications in the fields of industrial manufacturing and prototyping to increasingly find roles in scientific research contexts, such as synthetic chemistry. We present a general approach for the production of bespoke chemical reactors, termed reactionware, using two different approaches to extrusion-based 3D printing. This protocol describes the printing of an inert polypropylene (PP) architecture with the concurrent printing of soft material catalyst composites, using two different 3D printer setups. The steps of the PROCEDURE describe the design and preparation of a 3D digital model of the desired reactionware device and the preparation of this model for use with fused deposition modeling (FDM) type 3D printers. The protocol then further describes the preparation of composite catalyst–silicone materials for incorporation into the 3D-printed device and the steps required to fabricate a reactionware device. This combined approach allows versatility in the design and use of reactionware based on the specific needs of the experimental user. To illustrate this, we present a detailed procedure for the production of one such reactionware device that will result in the production of a sealed reactor capable of effecting a multistep organic synthesis. Depending on the design time of the 3D model, and including time for curing and drying of materials, this procedure can be completed in ~3 d.

INTRODUCTION

3D printing (or additive manufacturing) is a technique that fabricates physical objects from digital models by additive processes whereby successive layers of material are deposited to produce the final object¹. The development of these technologies began in the mid-1980s (ref. 2), but the use of 3D printing has expanded greatly in the past decade, moving beyond the preserve of industrial manufacturing and prototyping applications and promising to transform the relationships between the design, manufacture and operation of functional devices. Among the factors driving this growth has been the adoption of ‘open-source’ type development, which allows the creative adaption of the methods and the open sharing of expertise and innovation. Through the use of this approach, 3D printing has been exploited in a number of innovative ways to produce materials and functional devices. Notable among these new applications of the technology are the areas of medicine and biology, in which the ability to precisely place material in three dimensions has enormous worth in the fields of surgery³ and tissue engineering^{4–6}. 3D printing technologies have been used to construct scaffolds for cell growth^{7–12}, to build models of biological systems such as vascular networks^{13,14} and even to produce medical implants^{15,16}. Of particular interest to our group is the significant impact that the specific manufacturing capabilities of 3D printing technologies, along with the automation that they represent, could have on the chemical sciences^{17,18}. 3D printers are particularly attractive in this field, as their method of fabrication allows precise control over the topology, geometry and composition of the resulting reactor; we have termed this concept in reactor design ‘reactionware’ (Fig. 1)¹⁹. Key to this is the ease of use, versatility and economy of the new generation of 3D printers, which places the control over the context of the synthetic reaction in the hands of the direct user and allows reactor design to become an integral part of the experimental design stage of chemical synthesis. We have previously produced reactionware that was used for the synthesis of inorganic

polyoxometallate cluster materials, as well as organic phenanthridine derivatives¹⁹. The specific example described in this protocol results in the fabrication of a self-contained, sealed reactor that contains all the materials and reagents that are necessary for the synthesis of (1,4,5,6,7-pentamethyl-bicyclo(2.2.1)hept-2-ylmethyl)-phenyl-amine²⁰. The power of 3D printing lies in the versatility of applications in which it can be used, and the diversity of materials that are available for printing, meaning that no single protocol can encompass all the possible applications of this technology. With this in mind, we present a general introduction to 3D printing techniques, their limitations and the general design principles that are useful in the context of reactionware fabrication. Following this, we provide a protocol to exemplify these design strategies for the specific example of a sealed reactor that facilitates a multistep organic synthesis in which the reagents, catalysts and purification are integrated into the fabrication of the device²⁰. The protocol describes the preparation of the 3D model files that are necessary for the fabrication of the reactionware device, along with potential modifications to these files to achieve multicomponent fabrication. We then describe the use of two complimentary 3D printers (one for the inert thermopolymer architecture of the device and a second for composite catalyst materials, the preparation of which is also detailed) to complete the fabrication of the reactionware device. Finally, the protocol describes the addition of such non-printable materials (chemical starting materials and purification materials) that are necessary to produce the completed reactionware device.

Comparison of 3D printing methods

Before discussing the current state of the art for the application of 3D printing to the chemical sciences, it is worth briefly defining the several widely used types of 3D printing along with their basic principles and principal limitations. The range of 3D printers

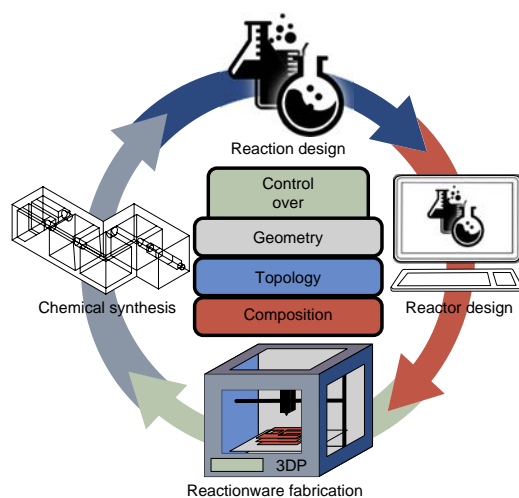


Figure 1 | Schematic representation of the concept of ‘reactionware’. 3D printing technologies are used in an iterative process whereby the needs of the chemical experiment inform the specific design and fabrication of the reactor device. Experimental results can then be rapidly fed back into the reaction and reactor design. 3D printing allows the end user to have unprecedented control over the geometry, topology and composition of the resulting reactor.

available is constantly expanding, which permits the printing of a broad and ever-increasing range of materials and allows the fabrication of devices that incorporate functional materials as an integral part of their structure^{21–24}.

The first commercialized type of 3D printing was stereolithography (SL), which is still a very widely used process²⁵. There are a number of different technical approaches to SL; however, the basic principle of the method is that a base that is submerged in a vat of photoactive, curable resin (most commonly either epoxy or acrylate based) is illuminated using UV light in such a way that a single layer of resin is cured before the base is moved, thus covering the printed layer with a fresh layer of resin. The process is then repeated until the object is complete. This method constrains the material from which the objects can be printed to the products of photopolymerization reactions, although some work has been done on incorporating active materials into the resin matrix to provide the final structure with active properties, which can be used for postprint modifications and so on²⁶. SL printers are traditionally expensive; however, more economical desktop models that are suitable for laboratory use are becoming increasingly available, along with low-cost systems that are designed specifically for research environments, and developments such as the use of two photon polymerization mean that the resolution that this method can achieve is high relative to that of other techniques^{27–29}.

A second paradigm of 3D printing is the use of ink-jet printing³⁰ either to directly print patterns of a photocurable resin layer by layer, which are individually treated by UV irradiation, or to print a binding material onto a layer of powder³¹, which is then covered by another layer of powder to repeat the process. As the direct printing method is related to the SL approach above, it shares the material limitations of that method. In contrast, the powder-based ink-jetting techniques give access to a broader range of materials, from polymers such as nylon to ceramics and glasses, leading to the use of this technique for biological scaffold generation^{32,33}

and drug delivery studies^{34,35}. However, the material properties of the resulting objects are usually dominated by the binding agent used.

Related to this powder-based approach is the technique known as selective laser sintering (SLS) whereby a high-powered laser is used to sinter powdered material (polymers³⁶ such as polycarbonate, polyvinylchloride, nylon, polyesters, metals³⁷ (such as titanium)³⁸ or ceramic powders³¹) in patterns to produce the desired object. This method can suffer from poor resolution and fidelity to the original design because of the intense local heating in which the laser melts the powder substrate and the subsequent cooling of the solidified material; the degree to which this affects the resulting structure depends on a number of parameters such as powder size, as well as focusing and power of the particular laser used³⁹.

Extrusion-based 3D printing techniques such as FDM are some of the most popular methods of 3D printing. This method in its most common form involves a movable heated print head that extrudes molten or semimolten material in predefined patterns onto a print bed. This bed is then moved incrementally in the vertical direction to allow the printing of subsequent layers. Although the resolutions offered by FDM are generally not as high as those afforded by the other methods mentioned, these printers are generally the most economical both in initial outlay and in terms of material costs (**Fig. 2**). A larger range of materials is available for this method (although not as wide a range as could potentially be used in SLS techniques), with the most commonly used polymers being polylactic acid and acrylonitrile butadiene styrene. The popularity of FDM printing, along with the adaptability of the technique (any material with a melting point in the range of the printer’s extruder and the correct flow characteristics has the potential to be developed for this method), mean a wide range of materials have been developed, including composite materials²². If the definition of FDM is expanded to include all extrusion-type 3D printing, then the range of materials becomes wider still, thus allowing any suitably viscous material to be printed.

The major application for 3D-printed devices in the field of synthetic chemistry that has been explored to date is in the area of fluidic reactors⁴⁰, especially as a parallel methodology to the more laborious and widespread soft lithography techniques. 3D printing offers an alternative approach to the creation of microfluidic devices either by providing a sacrificial scaffold for processing by traditional soft lithography using a curable resin such as polydimethylsiloxane⁴¹ or by directly printing fluidic channels by a 3D printing method. Indeed, research in our group has developed devices that interface with standard laboratory pumping/valving equipment to produce efficient and cost-effective fluidic reactors ranging from millifluidic^{42–44} to microfluidic dimensions⁴⁵. The fabrication of such devices is achievable in the scope of the present protocol. These approaches do not yet approach the resolutions and small channel sizes that are achievable by traditional microfluidic methods; however, this is an area of active research, and these resolutions are expected to improve in the near future, opening the prospect of true microfluidic-scale 3D printing. Beyond this application, 3D printing research in the chemical sciences has focused on the development of materials for 3D printing^{8,23,24,46–52}, postprinting modification of 3D-printed materials and their application to printed chemical or electronic devices such as batteries^{53,54} and LEDs²³.



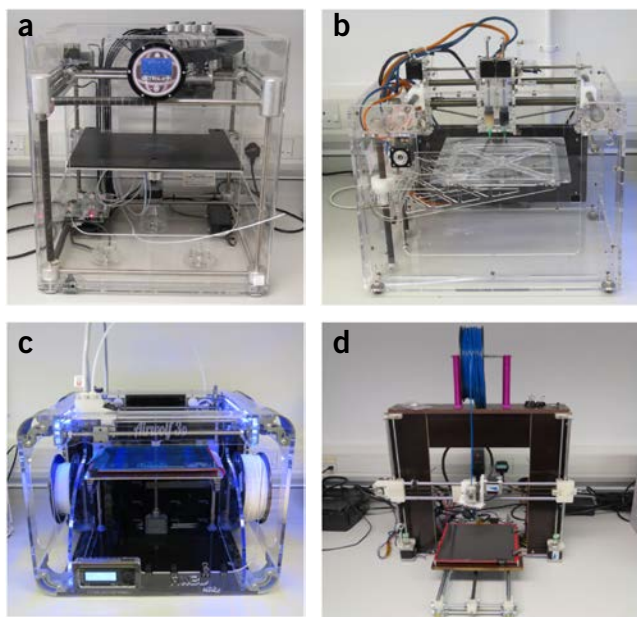


Figure 2 | Bench-top FDM and extrusion-based 3D printers used by the authors. (a) 3D Touch 3 extruder 3D printer, capable of printing a variety of thermopolymer materials, including polypropylene (PP). (b) Fab@Home Version 0.24 RC6 freeform fabricator syringe extrusion printer, capable of printing a range of viscous materials such as acetoxy-silicone polymer and composite catalyst materials. (c) Airwolf HD2X 3D printer, another example of a commercially available FDM printer that is capable of printing PP, which can be used as a suitable substitute for the 3D Touch in the presented procedure. (d) RepRap prusa i3 model assembled from a kit by the authors. Many open-source FDM 3D printers are available, the majority of which require assembly. These printers can act as substitutes for commercially available machines while also offering more scope for modification to suit particular experimental requirements, such as modifications to allow liquid handling or combined FDM and extrusion printing on one machine.

Limitations of 3D printing methods

The nature of each distinct 3D printing technique also entails certain limitations, especially when using 3D printing as a tool for use in synthetic chemistry. First among these are limitations imposed by the nature of the materials used. For example, the epoxy- or acrylate-based photopolymers used in SL and some ink-jetting processes tend to have very low resistance to many standard commonly used organic solvents, and they exhibit susceptibility to extremes of pH, thus severely limiting the application of these techniques in chemical applications. Similar problems arise when considering the thermopolymers used for standard FDM 3D printing, polylactic acid and acrylonitrile butadiene styrene. These generally show very poor resistance to organic solvents and/or acidic and basic conditions, which makes them unsuitable for large numbers of chemical applications. However, FDM printers can also be used with more chemically inert materials such as nylon and polyolefins. Ideally, perfluorinated thermopolymers would provide even greater chemical resistance than polyolefin-based substrates; however, the physical properties of these materials are not so well suited for printing. For example, polytetrafluoroethylene has a melting point of 600 K, and decomposition begins around 623 K, giving a very small temperature window to work in, and with the potential of producing extremely toxic decomposition

products. These solvent constraints do not pose so many problems for biological applications, which are largely conducted in aqueous media and at mild pH ranges; hence, 3D-printed labware is more common among such applications.

As described above, the FDM method of 3D printing used for the major structural elements of the devices is based upon the extrusion of molten thermopolymers. This process provides the resultant structure with an effective upper temperature limit above which the device will begin to lose its structural integrity. For PP, this limit is reached at ~160 °C, when the polymer begins to soften before melting. Many commercial FDM 3D printers contain polytetrafluoroethylene sleeves as part of the extruder assembly, which gives them a maximum working temperature in the region of 260 °C, although all-metal extruders, which have considerably higher working ranges, are becoming increasingly available. Other 3D printing techniques such as SLS and some powder-based ink-jetting methods can print high-temperature materials such as metals and ceramics, but these often require extensive postprinting treatment to minimize the porosity of the structures produced.

Another limitation that the manner of 3D printing imposes on the resulting structures is the useful geometries that the specific technique allows. For example, it is extremely difficult to use powder-based techniques such as SLS and powder-based ink-jetting to produce very small channels, as the complete removal of excess, unsolidified material is impossible. Therefore, these techniques cannot be used to produce geometries with internal voids, as these would be filled with untreated powders. Similar restrictions exist for some photopolymer-based techniques. However, FDM techniques do not have this limitation, and if they are carefully designed this technique can easily produce small fluidic channels along with internal voids, which can additionally be filled with secondary materials, such as chemical reagents, during the printing process.

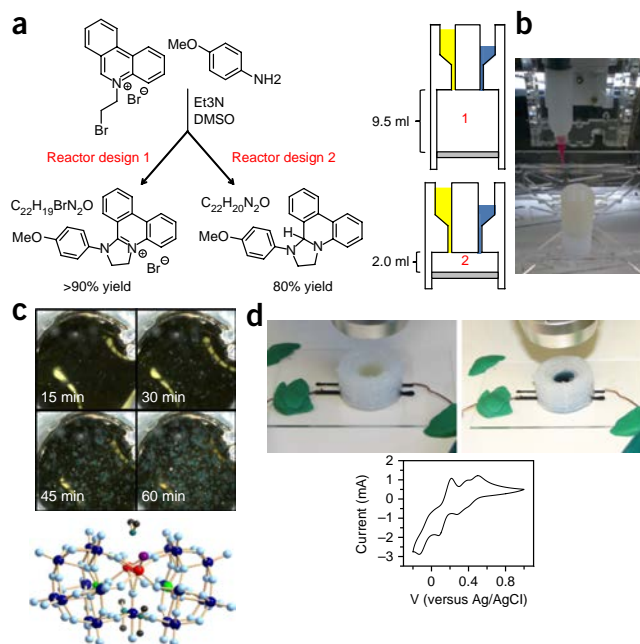
One of the major limitations of 3D printing in the production of fluidic reactionware devices is the difficulty that most 3D printing techniques have in producing moving parts such as valves and actuators^{55,56}, meaning that such reactionware must be interfaced with external valves, in contrast to some microfluidic techniques in which the flexibility of polydimethylsiloxane has been used to construct valves and even pumps on the microfluidic scale⁵⁷.

Applications of the method

In developing the concept of 3D-printed reactionware, we have previously shown that it is possible to use inexpensive materials to produce synthetically useful devices that incorporate active materials^{19,20}. By using an acetoxy-silicone polymer as a viscous printable matrix, we used a 3D printer to fabricate a variety of reactors (Fig. 3) that were used to synthesize inorganic polyoxometallate clusters (Fig. 3c), as well as perform standard organic syntheses. (Fig. 3a) The use of silicone rubber as the printing material also had the advantage of allowing the walls of the reactionware device to act as a self-sealing septum for the introduction of chemical reagents. It was shown during these experiments that the outcome of the synthetic procedure could be controlled by the geometry of the reactor itself, using the design of the reactor to influence the stoichiometry of the resulting reaction. Further, we showed that the resulting devices were suitable for use as electro-chemical reactors and that additives could be introduced to the print matrix



Figure 3 | Examples of reactionware printed with acetoxy-silicone polymer and composites thereof. **(a)** Reactor-geometry-controlled synthesis of $C_{22}H_{19}BrN_2O$ or $C_{22}H_{20}N_2O$. Altering the reactor geometry influences the outcome of the reaction; in reactor (1), two equivalents of 5-(2-bromoethyl)phenanthridinium bromide solution are allowed to mix with a *p*-methoxy aniline solution, thus allowing complete oxidation of the product to $C_{22}H_{19}BrN_2O$ with a yield of 90%, whereas the smaller volume of reactor (2) constrains the stoichiometry to 1:1, allowing the isolation of the unoxidized $C_{22}H_{20}N_2O$ species in an 80% yield. **(b)** Completed acetoxy-silicone-based reactionware ready to be removed from the printer for use. **(c)** Top: photographs of the crystallization of $(C_2H_8N)_7Na_4[W_{19}Co_2O_{61}Cl(SeO_3)_2(H_2O)_2]Cl_2 \cdot 6H_2O$ at various times after the initial mixing in a reactionware device fabricated with a nonprinted glass slide as a viewing window. Bottom: ball-and-stick representation of $[W_{19}Co_2O_{61}Cl(SeO_3)_2(H_2O)_2]^{6-}$ with protons omitted for clarity. Black, teal, cyan, green, violet, dark blue and red represent C, N, O, Se, Cl, W and Co, respectively. **(d)** Top left: 3D-printed electrochemical cell using printed conductive printed acetoxy-silicone/carbon black composite electrodes filled with a 5-mM solution of phosphomolybdic acid (PMA) in 0.1 M H_2SO_4 before electrochemical reduction. Top right: the same cell after reduction at 22.5 V for 4,500 s. Bottom: cyclic voltammetry, recorded in acetoxy-silicone reactionware (not shown), for PMA (5 mM in 0.1 M H_2SO_4) at a scan rate of 0.1 V s^{-1} . Adapted with permission from Symes *et al.*¹⁹.



to achieve functional results—the incorporation of catalysts and conductive materials (Fig. 3d).

Building on this work, we have developed protocols for using the FDM method of 3D printing to produce structures in PP, which is a robust polyolefinic substrate that can withstand a broad range of chemistries. Exploitation of PP as a substrate has allowed the development of 3D printing as a laboratory tool for the production of otherwise specialized equipment such as self-contained millifluidic flow devices. These flow devices were used to explore a number of chemical systems, both as synthetic flow reactors (Fig. 4a–c) and as interfaces with in-line analytical techniques (Fig. 4b–f).

A further use of PP-only reactionware takes advantage of the FDM method of 3D printing to fabricate monolithic geometries that contain internal voids, thus allowing the production of hydrothermal reactors in which the reactants are introduced during the fabrication process and which can be tailored to the volumetric capacity required for the synthesis⁵⁸. These reactors do not require the stainless steel surround of traditional hydrothermal synthesis equipment, which markedly reduces the cost of such reactors and facilitates the economic production of high-throughput hydrothermal arrays for discovery purposes (Fig. 5). The limitation of temperature imposed by the PP material led to a restriction in the temperatures that are available for use in this hydrothermal reactionware to below 140 °C, where maintaining the mechanical strength of the device is paramount. The development of higher-temperature FDM 3D printers will have a significant impact on this area of reactionware.

We further combined these two approaches to produce multimaterial reactors that included both PP structures and acetoxy-silicone-based components. This combination permitted the production of devices that were robust to synthetic chemical conditions while also incorporating active materials such as a carbon-supported Pd catalyst and an acid catalyst (in this case Lewis acid montmorillonite clay), which were embedded in an acetoxy-silicone matrix to render them printable into the final structure. These designs also included multiple reaction

chambers in which mutually incompatible reactions could take place in a predesigned sequence to effect a continuous multistep synthesis involving three successive transformations on a core molecule (Fig. 6).

Experimental design

Overview of an example reactor. The reactionware used in this protocol consists of three separate reaction chambers that were designed in such a way that successive 90° rotations of the device will transfer the reaction mixture through the separate chambers as the reaction progresses, while ensuring that only the desired reaction occurs at any one time. These reaction chambers are preceded by two starting material chambers in which the initial reagents reside until the device is tilted by 45° to mix the reagents in the first reaction chamber. After the final reaction chamber is a short column that is manually filled with silica during the printing to provide a purification step to the reaction sequence (Fig. 6)²⁰.

File types. As 3D printing is a process that translates 3D models produced by a computer-aided design (CAD) software package (many such packages are available that provide varying levels of functionality, corresponding to the level of expertise required to use; examples of such packages are AutoCAD, FreeCAD, Rhino and so on) into a physical object, the original design is therefore crucial to the design of any experiment involving 3D-printed reactionware. Once the design has been created, it must be converted into an .stl file (defined as a stereolithography or Standard Tessellation Language file; the .stl file is accepted as the standard format for digital models used with 3D printing) that comprises information about the surface of each 3D object present as triangular sections, whose vertices are defined as Cartesian coordinates. The resolution of the digital model is therefore defined by the number of these triangles, with more triangles present allowing greater resolution of, for example, curved surfaces. These .stl files are then translated (‘sliced’) into a series of horizontal cross-sections, the thickness of which depends on the type of printer used. These cross-sections are then used to define the patterns that

PROTOCOL

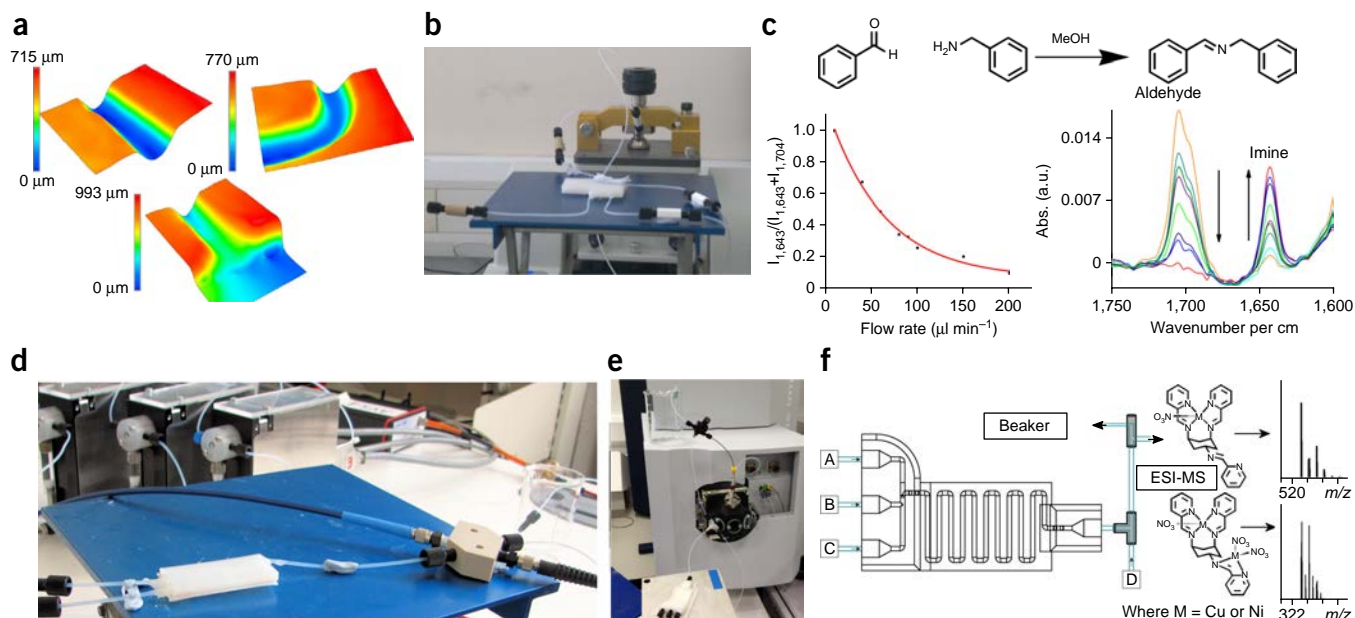


Figure 4 | 3D-printed reactionware used for fluidic applications in conjunction with in-line analytics. **(a)** 3D profiles obtained by optical microscopy of fluidic channels printed in PP for use in fluidic devices. Top left: a typical straight channel section. Top right: a 90° bend in a channel. Bottom: external channel opening at the wall of the device. All printed channels exhibited a consistent diameter of ~0.8 mm. **(b)** One such 3-input-1-output fluidic device connected to input pumps, with the output channel connected to an in-line ATR-IR flow cell. **(c)** Flow synthesis of a simple imine characterized by intensity of aldehyde versus imine characteristic peaks measured using flow ATR-IR at various reactor residence times. **(d)** 2-Input device connected to an in-line flow UV-visible cell. **(e)** 3-Input-1-output fluidic device interfacing with electrospray ionization–mass spectrometry (ESI-MS). **(f)** Continuous parallel analysis of the complexation of Cu²⁺ or Ni²⁺ with *cis,trans*-1,3,5-tris(pyridine-2-ylmethyl-ene)cyclohexane-1,3,5-triamine using the 3D-printed flow device. **a–d** adapted from Kitson *et al.*⁴⁴; **e, f** adapted from Mathieson *et al.*⁴², Beilstein *J. Nanotechnol.* (© 2013 Mathieson *et al.*; licensee Beilstein-Institut).

the 3D printer will need to generate for each layer, and a printer instruction file (generally known as a ‘G-code’ file after the particular programming language used) is generated that is specific for an individual make and model of printer. There are a number of programs available for translating .stl files into printer instruction files; some of these are proprietary of the 3D printer manufacturer, and others are open-sourced and can produce instruction files for a number of different printers (two of the most popular of these programs are Slic3r (<http://slic3r.org/>) and Cura (<https://ultimaker.com/en/products/cura-software>), which can produce instruction files for a broad range of FDM printers).

Considerations on the geometry and topology of the reactor.

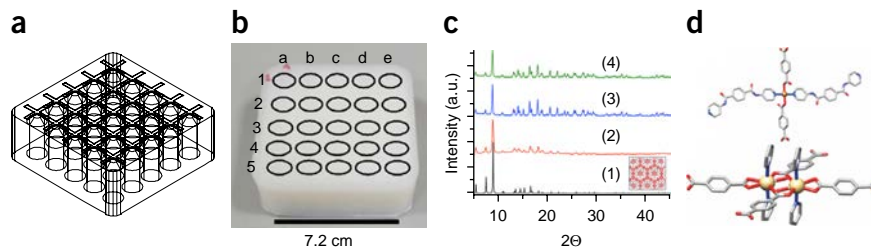
As discussed above, producing reactionware through 3D printing techniques gives the experimenter control over the geometry, topology and composition of the resulting reactor, and as such

the experimental design must consider each of these aspects with respect to the purpose of the given reactor.

The geometry of the reactor can be regarded as the specific size and shape of the final object. When considering the geometry of reactionware, it is important to bear in mind the basic principle that underlies 3D printing: it is a process for manufacturing solid objects by building up successive layers of material. This principle implies a number of basic design policies that should be adopted to make the most of the abilities of any 3D printer; for example, very often the resolution of a 3D printer will be much higher in the *z*-axis—that is, the vertical direction of printing—as this axis is required to move only very small increments in only one direction. In comparison, the *x*- and *y*-axes will be required to move much larger distances both forward and backward. The particular resolutions will vary from printer to printer; however, if small features are required that approach the limit of the printer’s

Figure 5 | 3D-printed reactionware for high-throughput hydrothermal screening applications.

(a) 3D CAD model of a monolithic 5 × 5 array hydrothermal reactor with chambers of 1-ml capacity for discovery-scale reaction screening. **(b)** Fabricated hydrothermal reactor array, filled during a pre-programmed pause in the 3D printing process; rows 1–5 and columns a–e were used to systematically vary reaction conditions over a number of reaction systems. **(c)** Powder



X-ray diffraction patterns of literature metal organic framework (MOF) MIL-96 (ref. 59): (1) calculated from single crystal X-ray structure, (2) obtained from a 3-ml-capacity 3D-printed hydrothermal reactor, (3) obtained from a 20-ml capacity 3D-printed hydrothermal reactor and (4) obtained from traditional hydrothermal equipment. **(d)** Top: ball-and-stick representation of the primary coordination environment of Cu²⁺ in [Cu(C₈H₄O₄)(C₁₈H₁₅N₄O₂)]_n. Bottom: ball-and-stick representation of the dimeric Cd²⁺ subunit of [Cd(C₈H₄O₄)(C₁₈H₁₅N₄O₂)]_n; two MOF materials discovered using the array reactors depicted in **a** and **b**. Orange, yellow, blue, red and gray represent Cu, Cd, N, O and C, respectively. Adapted with permission from Kitson *et al.*⁵⁸.

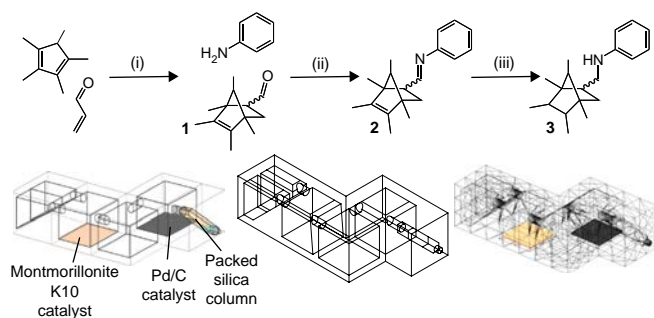


Figure 6 | The design and function of the reactionware device for which fabrication is described in this protocol. Top: the reaction for which the example reactionware used in this protocol was designed: (i) the acid-catalyzed Diels–Alder reaction of 1,2,3,4,5-pentamethylcyclopentadiene with acrolein to form a bicyclic bridged structure with pendant aldehyde group, **1**. (ii) This aldehyde group is then reacted with aniline to form imine **2**. (iii) The resulting imine is catalytically reduced over a Pd/C bed using triethylsilane as a hydride source to give the final product **3**. Bottom: design process for reactionware to accomplish the chosen reaction sequence; left: schematic diagram of reactor concept; middle, CAD model incorporating design principles discussed for FDM reactionware fabrication. Note, for example, the bevelled edges at the top of the reaction chambers, which enable the printing of the roof sections by reducing the distance required for the PP printing to bridge over. Right: rendering of resulting .stl files ready for 3D printing.

resolution, it is best to design the object such that the orientation of the model permits the required resolution. It is best also to design your objects to minimize the need for support materials, which means that the angle from the vertical of overhanging areas should be kept smaller than 45° if possible, as above this angle the preceding layers of the object will not be capable of supporting the subsequent layers and the print will not maintain the designed shape. It is possible to produce overhanging features, as can be seen in the example used for this protocol; however, the exact implementation of these structures is not trivial, and it often requires many device re-designs based on failed prints to achieve the final product. As 3D printing is a layered method of construction, the mechanically weakest part of the finished object will be the adhesion between the constituent layers of the printed device, and excessive stress in this direction may lead to delamination of the layers of the device leading to possible leakages and failures. This means that when designing any reactor that will experience elevated levels of mechanical stress (such as the post-printing incorporation of screws in the design, which will exert force in a defined direction), it is, if possible, advisable to orient the design while printing such that these stresses are exercised horizontally rather than vertically in the device. The factors that are involved in the design of the geometry of any reactionware device will vary according to the particular 3D printer being used for the task, and often the manufacturers of 3D printers will provide their own equipment-specific design guidelines, which should be consulted along with the very general principles outlined here.

When these design principles are adhered to, the details of the geometry of the device being printed are determined by the specific use to which the experimenter wishes to put the resulting reactionware; the number, capacity and shape of any reaction chambers required, along with the specific dimensions of connecting channels, will be dictated by the needs of the experiment, such as the volume of reaction mixtures present, as well

as physical properties such as the surface tension of any solvents used in the experiment.

The topology of the reactionware device can be considered to be the connectedness of the features of the device, such as the number of inlets and outlets of any fluidic system, along with the interconnections of channels within the structure. The nature of 3D printing imposes very few constraints on this aspect of the design process, as long as the general design principles outlined above are adhered to. Another feature of 3D-printed reactionware, which differentiates it from standard labware manufactured remotely from the point of use, is the possibility of producing hermetically sealed, monolithic devices into which any and all required reactants, reagents and catalysts are added during the manufacturing process. This requires the designer to consider the equalization of pressure through the device, especially if liquid material is to be moved through narrow junctions. Any inputs or outputs of fluidic devices will need to be attached to external tubing and pumps. It has been proven to be possible to use standard fluidic fittings to produce a reliable solvent-tight seal with 3D-printed devices⁴².

Choice of material. Control of the composition of the reactionware is achieved by varying the materials used to print the device. In general, it is necessary to choose a material that is inert to the desired chemistry as the main structural element of the device. This material should also be sufficiently resistant to any solvents, acids or bases that will be present during the duration of the experiment, so that the integrity of the device is maintained. In our case, PP was chosen, as it provides a balance between ease of printing, resolution of printing and chemical inertness, which enables it to act as a passive container to a wide range of chemistries. PP is, however, not completely inert, and it can be attacked by very strongly oxidizing agents and by prolonged exposure to solvents such as toluene at elevated temperatures.

Incorporation of nonprinted parts. Further considerations of the composition of the reactionware are whether the device is to incorporate nonprinted parts that must be inserted into their correct positions either during or after the printing process, in which case the space required for these pieces to fit securely in the desired position must be calculated and incorporated in the design of the device. Such nonprinted pieces could include LEDs, conductive wires, windows through which spectroscopic or visual observations could be made, or items that are impossible to print in the regime being used for the rest of the device, such as sintered glass used for filtering solutions. These items also require that the printing be paused to allow the insertion of the object; these pauses can be automated at the stage of preparing the printer instruction file.

Printing with multiple materials. It is also possible to print in more than one material to complete the fabrication of reactionware devices. These separate materials can be other thermopolymers on the same 3D printer as is being used for the majority of the printing, or the partially completed print can be transferred to a separate printer for printing of an alternate material. The latter is the approach used for our protocol, in which we were required to use an alternate, extrusion-based 3D printer for the printing of viscous curable acetoxy-silicone-based composite materials.

PROTOCOL

These materials were produced using catalysts that were specific to the reactions chosen for the particular reactionware device; however, there is vast scope for the development of further catalyst-based composite materials or even the printing of reagents in this form.

Printing using multiple materials imposes certain design constraints upon the reactionware device; with most current 3D printing software, areas to be printed in each individual material must have their own separate .stl file, which should be created as having the same origin point so that each material is printed correctly in relation to the initial design. If this involves transfer of the print between printers, it is vital to ensure that each printer is calibrated correctly and that the print being transferred is oriented precisely on each printer before printing commences; the potential for error in this process is great, and therefore the need for transfers between printing apparatuses should be kept to a minimum at the reactionware design stage. Pre-programmed pauses can be inserted into the printer instruction file at specific points through the print, either by manually altering the G-code instructions or by using software during the production of the printer instruction file. Another consideration in the printing of multiple-material prints is the compatibility of the materials used to print—for example, the choice of PP as a structural element

has advantages in terms of chemical compatibility and robustness; however, PP's low surface energy means that very few other materials will adhere easily to the surface and vice versa.

Choice of printer. As can be seen, the process of 3D printing is linked inextricably with the exact printer or printers being used. The equipment will define the parameters, such as maximum build size, resolution and material options, within which the user can design the desired reactionware. 3D printing is a rapidly developing technology, and the turnover of commercially available equipment is relatively high, with 3D printers regularly being replaced by updated models. This makes the creation of a universally applicable procedure virtually impossible. Indeed, the following protocol was developed on one such discontinued printer, the 3DTouch 3 extruder 3D printer. However, we have attempted to tailor the protocol such that the steps described will be similar for any suitable equipment, and PP printing should be feasible on any FDM-type printer that is capable of printing to at least 240 °C. The other printer used in the procedure for catalyst material printing, the Fab@Home Version 0.24 RC6, was developed as an open-source project and thus may not be widely available in the exact configuration used in this protocol, but once again alternate setups can provide the same functionality.

MATERIALS

REAGENTS

- Polypropylene (PP) rod—3-mm-diameter circular profile (individual grades of PP may require slightly different print settings because of variations in their melt profiles and flow characteristics. The PP used by the authors for the protocols described was supplied by Barnes Plastic Welding Equipment. BB2 4AJ product code: WR.PP3.NT.2.B)
- Acetoxy-silicone polymer—LOCTITE 5366 bathroom sealant, Loctite
- Pd/C 10% (wt/wt) (CAS 7440-05-3, Sigma-Aldrich, item number 520888)
- Montmorillonite K10 powder (CAS 1318-93-0, Sigma-Aldrich, item number 69866)
- Toluene, reagent grade (CAS 108-88-3, Sigma-Aldrich, item number 179418) **! CAUTION** Toluene is highly flammable and is an irritant, and its vapors may cause drowsiness and dizziness.
- *n*-Hexane, reagent grade (CAS 110-54-3, Sigma-Aldrich, item number 208752) **! CAUTION** *n*-Hexane is highly flammable and is an irritant; it is harmful and dangerous for the environment and toxic for reproduction.
- Diethyl ether, reagent grade (CAS 60-29-7, Sigma-Aldrich, item number 676845) **! CAUTION** Diethyl ether is highly flammable; it may form explosive peroxides, and vapors may cause drowsiness and dizziness.
- 1,2,3,4,5-Pentamethylcyclopentadiene, 95% (CAS 4045-44-7, Sigma-Aldrich, item number 214027) **! CAUTION** This compound is flammable.
- Acrolein, 90 % (CAS 107-02-8, Sigma-Aldrich, item number 110221) **! CAUTION** Acrolein is flammable, is an irritant and is corrosive.
- Triethyl silane, reagent grade (CAS 617-86-7, Sigma-Aldrich, item number 230197) **! CAUTION** Triethyl silane is flammable.
- Aniline, reagent grade (CAS 62-53-3, Sigma-Aldrich, item number 242284) **! CAUTION** Aniline is toxic by inhalation, on contact with skin or if swallowed, and it is a possible carcinogen and may cause sensitization; it is toxic for the aquatic environment.
- Celite 535 (CAS 68855-54-9, Sigma-Aldrich, item number 22138)
- Silica gel, technical grade, pore size 60 Å, 200–425 mesh particle size (CAS 112926-00-8, Sigma-Aldrich, item number 645524)
- Glass wool (Fisher Scientific, product code 10024923)

EQUIPMENT

- Bits from Bytes (BfB) 3DTouch 3 extruder 3D printer (Bits from Bytes, now part of 3DSystems <http://cubify.com/support/legacy/manuals/>)

- Fab@Home Version 0.24 RC6 freeform fabricator assembled from a kit by the authors (discontinued, <http://www.fabathome.org/>; an updated version of the platform is available at <http://fabstore.seraphrobotics.com/international.html>)
- Airwolf HD2X 3D printer (Airwolf3d, <http://airwolf3d.com/>)
- Polypropylene (PP) printing beds, 200 × 200 × 12 mm (many suppliers of cut plastic sheeting are available, and most will be able to supply sizes of PP sheets of appropriate dimensions to be suitable)
- Adhesive tape (duct tape type; any brand will do)
- USB storage disc (any will do)
- Micro SD storage card (any will do)
- Disposable PP sample containers (Fisher Scientific, product code 11739743, although any suitable container will do)
- 0.5-inch (1.27-cm) length straight cannula blunt-end dispensing tip, 18 gauge, 0.84-mm internal diameter (Fisnar, part no. 5601087)
- PP syringe barrels, 10-ml capacity (Fisnar, part no. 8001003)
- Appropriate 3D computer-aided design (CAD) software (the authors used a variety of CAD software in the preparation of this work, although any software package that is capable of exporting 3D designs in a .stl format would be suitable for this work, and a number of software packages are available such as, among others, proprietary software AutoCAD (<http://www.autodesk.com/>) and Rhinoceros (<http://www.rhino3d.com/>) and free, open-source alternatives such as OpenSCAD (<http://www.openscad.org/>; a parametric, script based package) and FreeCAD (<http://www.freecadweb.org/>)
- Software for converting .stl files into instruction files for 3D printers. Numerous programs are available for this task, some of which are proprietary of the 3D printer manufacturer

EQUIPMENT SETUP

3D printer There are generally two types of FDM 3D printers that can be used to achieve the results described in the following protocol: commercially available bench-top 3D printer suitable for printing PP (i.e., their extruders are capable of reaching at least 240 °C) and kit-based open-source 3D printing equipment.

Commercially available FDM 3D printers such as the 3DTouch used in the following procedure and the Airwolf HD2X printer, which can be used as an alternative, have manufacturer-specific setup instructions that must be followed to initially set up the printers, and they are often stand-alone

machines that do not require connection to a computer to function. These procedures are not laborious for such commercial machines, and the printers are generally ready to use 'out of the box', within a matter of hours. Once they are set up, all that is required is that the correct materials are installed in the machine in the correct place for printing. Commercial 3D printers can vary significantly in the degree of flexibility in control and use of materials available, and it is important to ascertain that the capabilities of any selected printer are consistent with the use to which it will be put before selection of equipment. The majority of FDM printers available will be able to achieve the results described herein with minimal modification; however, some will have designed restrictions that may make them unsuitable for reactionware synthesis.

Open-source and kit-based 3D printers such as the Fab@Home (<http://www.fabathome.org/>) printer used for viscous material deposition in this procedure and RepRap-type (<http://reprap.org/>) 3D printers generally require assembly before use. This means that it is possible to modify these printers extensively to tailor them for the specific applications as desired, but a degree of expertise in construction and electronics is required for this process.

The Fab@Home printer used in the following procedure was constructed from a kit by the authors without modifications from the original specifications. The building of 3D printer systems is outside the scope of the current work, and it varies greatly between models of 3D printer kits. This generally requires a significantly longer time to set up than commercial 3D printers, with some degree of expertise in electronics and mechanical assembly required to attain optimal results. These kit printers are often directly controlled by a USB connection to a dedicated computer running the printer-specific software (such as the Fab@Home software or other open-source programs such as octoprint (<http://octoprint.org/>) or printron (<http://www.pronterface.com/>) for RepRap-based systems). Specific modifications can be made to RepRap equipment to make it suitable for printing of the composite materials described in this work (http://reprap.org/wiki/Paste_Extrusion).

The model design stage and printer instruction file preparation require that suitable computers that are capable of running the required software be available.

No other equipment setup is required beyond that necessary for the general functioning of a standard synthetic chemistry laboratory.

PROCEDURE

Preparation of the print file ● **TIMING depends on the complexity of the design; these steps can be completed at any point before the required printing of the device**

1 | Design a 3D reactionware structure that is required for the purpose of the experiment. Prepare the 3D digital model of your reactionware using a suitable software package. AutoCAD 2014 has been used here, but other software packages are also available (**Fig. 7a**). The great flexibility of 3D printing provides very few constraints upon the geometries to be produced during the process; however, limitations of design because of the FDM method should be borne in mind when creating the design, as discussed in the Experimental Design section. Ensure that each section of the design that is to be printed in a separate material is available to be exported as separate .stl files. For the example shown in **Figure 6**, three stl files are produced (**Supplementary Data 1**): one for the PP architecture of the reactionware (Reactionware PP architecture.stl) and one each for the two catalyst beds (montmorillonite K10 (Montmorillonite composite.stl) and Pd/C composite acetoxy-silicone material (Pd composite.stl)) to be printed in chambers 1 and 3.

▲ **CRITICAL STEP** Separate parts of the object to be printed must be exported as .stl files with the same origin point to ensure their correct positioning in the final printed object. In general, it is not advisable to print more than three layers of material, which requires a change of printer consecutively (PP printer to soft material printer or vice versa), as the height of the printed material will interfere with the print head of the other printer when transferring the print back. If printing of complex 3D geometries of alternate materials is desired, this may necessitate several transfers of the ongoing print between printers to build up the desired geometries. The requirement for this should be kept to a minimum at the reactionware design stage, as each transfer between printers carries an additional risk of print failure (see TROUBLESHOOTING).

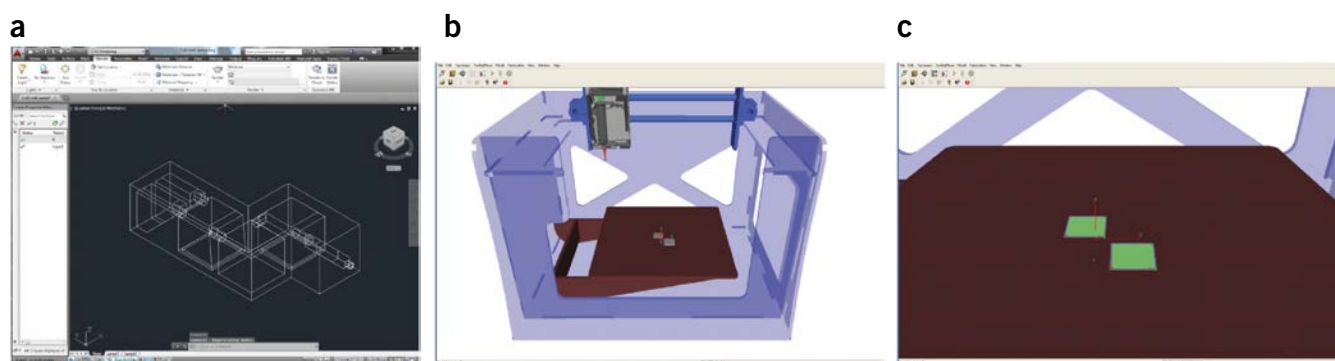


Figure 7 | Preparation of printer instruction files. (a) Step 1: preparation of 3D digital model of reactionware using a suitable software package; the example used here is AutoCAD 2014, but other software packages for this process are also available. (b) Step 3: import of the catalyst bed .stl files into the Fab@Home control software. (c) Step 4: after assigning the correct material for each catalyst bed, the software calculates the patterns in which material will be laid down to print the desired shape.

2| Export object part files as individual .stl files according to the procedure of the 3D CAD software.

▲ CRITICAL STEP Errors in the .stl file, such as nonwatertight meshes (i.e., the triangular mesh that defines the solid has a hole, which makes it hard for the software to determine the ‘inside’ and ‘outside’ of the solid object), which can arise at this stage because of complex geometries, can cause problems with the 3D printing slicing software in the next stage. It is advisable to check the validity of the .stl file after export. A number of freely available software programs are available for this, such as netfabb (<http://www.netfabb.com/>), which can identify and fix such .stl errors.

3| Import the .stl files for the design into the appropriate software for the 3D printers being used. In this case, the .stl file corresponding to the PP architecture was imported into the Axon 2.0 software for use with the 3DTouch 3D printer, and the .stl files corresponding to the catalyst beds were imported into the Fab@Home control software (**Fig. 7b**).

4| Ensure that the correct print settings have been applied for the material that will be printed. The optimal settings can vary depending on the grade of PP and the specific make and model of the 3D Printer being used. Ensure that, for any multimaterial prints, the correct material is assigned to the corresponding .stl file, and that this corresponds to the physical setup of the printer being used to ensure the printing of the correct material in the correct position.

▲ CRITICAL STEP The settings used for printing will determine the physical properties of the object printed; the wrong settings will lead to an object that does not conform to the original design or potentially does not function as desired (e.g., leaking devices or blocked channels). We have provided a general discussion on the importance of print settings in the **Supplementary Discussion**.

? TROUBLESHOOTING

5| Convert .stl files into 3D printer instruction files, using the appropriate process for the software being used. At this stage, the print file will require to be modified to incorporate any pre-planned pausing in the print process in order to change the printer or to incorporate nonprinted components into the reactionware device being fabricated. This process is different depending on the type of 3D printer being used. If the conversion software allows this as part of the standard conversion process, proceed with option A. If not, it will be necessary to proceed with option B to modify the printer instruction file.

(A) The 3D printer conversion software allows this as part of the standard conversion process

▲ CRITICAL STEP The following exact procedure is described for plugins in the free, open-source software Cura 15.02.01; this program was initially developed by 3D printer manufacturer Ultimaker, and it is capable of producing printer instruction files for a wide range of FDM-type 3D printers.

- (i) Identify the precise height or layer at which the pause is required.
- (ii) In the ‘Plugin’ section of the Cura user interface, use the ‘Pause at height’ plugin to introduce a pause at the appropriate point.
- (iii) Use the ‘Tweak at z’ plugin to adjust the print temperature for the two layers subsequent to the pause up by 20 °C to ensure correct layer adhesion after print resumption.
- (iv) Save the resultant printer instruction (G-code) file.

(B) The printer conversion software does not allow the insertion of pause commands as part of the conversion process

▲ CRITICAL STEP In this case, it is necessary to modify the printer instruction file once it has been created (the following procedure is described for the G-code file produced by the 3DTouch 3D printer software, Axon, as used by the authors. Other 3D printers may use other G-code commands to achieve similar results; a repository of G-code commands for various makes and models of 3D printers can be found on the RepRap website (<http://reprap.org/wiki/Gcode>).

- (i) Process the desired .stl file into a printer instruction (G-code) file and save the resultant file.
- (ii) Open the printer instruction file using a text editor application such as Notepad or similar. An example print instruction file is provided as **Supplementary Data 2**.
- (iii) Identify the lines of G-code, which corresponds to the precise layer after which the pause is required. This can be done efficiently by using the ‘find’ function in the chosen text editor program and searching for the z coordinate (i.e., height) of the layer—for example, ‘Z26.33’ to find the lines of code that refer to the layer printed at 26.33 mm above the print bed. The modifications to the code should be added after these instructions.
- (iv) After the appropriate line, insert the code as follows (each command should be given a separate line in the instruction file; comments are added for clarity and should not be included in the file).

Command	Description
M542	This command is used to return the print head to its resting position
M226	This command instructs the printer to pause until user input resumes the print
M104 S260	This command sets the extruder temperature for extruder 1 (for extruder 2 use M204, for extruder 3 use M304) to a temperature of 260 °C—i.e., a temperature 20 °C higher than the previous printing temperature
M543	This command instructs the printer to exit the resting position once the temperature has reached the set point

- (v) Identify the lines of G-code that correspond to the precise layer to be printed two layers subsequent to the pause (i.e., two increments of the z-layer height identified in the specific print settings being used for the make and model of printer). For example, if the print is paused before the layer corresponding to a z-axis height of 4.5 mm and each layer is 0.125 mm in height, then the following code should be inserted before the layer deposited at a z-height of 4.75 mm.
- (vi) After the appropriate line, insert the code as follows (the exact function of each command is as described in the table above; these commands are used to reset the print temperature to the original value):

```
M542
M104 S240>
M543
```

- (vii) Save the resultant printer instruction (G-code, suffixed 'bfb') file.

? TROUBLESHOOTING

6| Transfer the printer instruction file to a storage medium ready for transfer to the appropriate 3D printer—for example, a USB storage disc for the 3DTouch. The Fab@Home printer is directly controlled through a USB cable connection to a suitable PC, and thus these files do not need to be transferred to storage medium.

■ **PAUSE POINT** At this stage, the printer instruction files can be stored indefinitely before being uploaded to the 3D printers being used. A reactionware design can go through many iterations before any physical printing takes place.

Preparation of PP 3D printer ● TIMING 20 min

7| Ensure that the PP filament is correctly inserted in the machine. The exact procedure for this will depend on the make and model of the 3D printer being used (see Equipment Setup above); the manufacturer's guidelines should be followed.

8| Place and position appropriate print bed. In order to print PP successfully, it is necessary to use a PP surface as the substrate for printing. Affix a square board of PP at least 10 mm thick (the authors use 12 mm) to the print bed of the 3D printer using a suitable adhesive tape. Depending on the particular printer being used, it may be necessary to preheat the print bed to above ambient temperature to obtain suitable adhesion of the material to the print bed. If this is the case, mechanical clips may be necessary in place of adhesive tape, which must be placed so that they do not interfere with the motion of the print head. Preheating can add significant time to the printer preparation.

▲ **CRITICAL STEP** If the print is to be transferred to a second printer for the introduction of soft material components such as catalyst-loaded acetoxy-silicone polymer, it is vital to precisely position the print bed such that it can be replaced at exactly the same point to facilitate the subsequent resumption of PP printing. This process must be performed on all 3D printing devices used in the fabrication of the reactionware, and it is vital that the print bed be positioned on each machine such that the origin of each machine is at the same place on the print bed to ensure that printing of each component is in the correct position. The most convenient way of doing this is to identify the center point of each printer's print area by moving the print head using the printer's control software and by carefully aligning this with the center point of the print bed.

? TROUBLESHOOTING

9| Adjust the origin z-height of the printer to ensure that the print begins on the newly affixed PP bed. This is a setting that is adjustable on the printer itself, and it usually requires that the print head be moved to the center of the print area and the height of the print bed be either mechanically changed by means of adjustment screws or adjusted using the control options on the printer's user interface (as in the case of the 3DTouch machine). The print head should be adjusted so that the extruder nozzle sits between 100 and 200 μm above the surface of the print bed. Smaller distances will result in better adhesion to the print bed, but they can cause problems in removing the finished object from the bed, whereas larger distances will facilitate removal from the bed but can cause increased risk of warping and detachment during printing (see TROUBLESHOOTING).

? TROUBLESHOOTING

10| Level the print bed by moving the print head into each of the four corners of the print bed and using the printer's adjustment screws to ensure that the extruder nozzle is at the same height above the print bed in each position.

11| Return the print head to its standby position ready to begin printing.

Printing of PP parts of the reactionware device ● TIMING 2 min + printing time (depends on size of device; generally several hours)

12| Insert the storage device (USB or Micro SD card) into the printer and use the printer's controls to select the desired file (as prepared in Steps 1–6) for printing.

PROTOCOL

13| Initiate printing of the desired file.

14| Observe the initial stages of printing to ensure correct and secure adhesion to the print bed. If the printed piece appears to be insecurely attached to the print bed, it may be necessary to abort the print and remove any deposited PP before repeating Steps 9–11 to adjust the print bed z-height and level.

! CAUTION The extruder of the 3D printer will become very hot during printing, and care should be taken that the printed material and extruder have cooled sufficiently before it is handled.

15| Observe the printer periodically through the print process to ensure that the fabrication is proceeding according to the design with no errors. There are a number of ways that the printing process can fail at this stage (see TROUBLESHOOTING).

? TROUBLESHOOTING

■ PAUSE POINT At this stage, the 3D printer can generally be left printing until the pre-programmed pause in the printing process, at which time the 3D printer will require intervention to restart printing. It is generally not advisable to leave the 3D printer in this state for extended periods of time, but modest delays of up to 3–4 h are acceptable.

Preparation of composite catalyst materials for printing ● TIMING 10–15 min

▲ CRITICAL Steps 16–20 should be carried out as close to the material's use time as possible, as the acetoxy-silicone polymer begins to cure as soon as it comes into contact with atmospheric moisture; if the material is prepared too far in advance, the printing characteristics of the composite material will be impaired and fresh material will have to be prepared.

16| Assemble the required materials for the preparation of composite soft materials for printing.

17| Deposit 4.2 g of acetoxy-silicone polymer into a suitable receptacle (the authors use 25-ml capacity disposable PP containers; **Fig. 8a,b**), followed by 2.0 ml (~1.7 g) of toluene. Mix this using a glass stirring rod until a homogeneous mixture is obtained (**Fig. 8c**). Care should be taken during this process to ensure that as few air bubbles as possible are introduced to the mixture, as these can impede the smooth flowing of the material during printing.

! CAUTION Organic solvents such as toluene should be handled using appropriate protective equipment such as nitrile gloves and lab coats, and they should generally be carried out in an extracting fume hood.

18| To this mixture, add the desired quantity of additive for the specific type of application required. To produce composite materials loaded with (i) 10 % Pd/C catalyst (**Fig. 8d**) suitable for effecting the catalytic reduction of alkenes and (ii) montmorillonite K10 Lewis acid clay, which has been used to catalyze Diels-Alder cyclizations, add 0.5 g of the desired additive to the acetoxy-silicone/toluene mixture and thoroughly blend it until a homogeneous mixture is

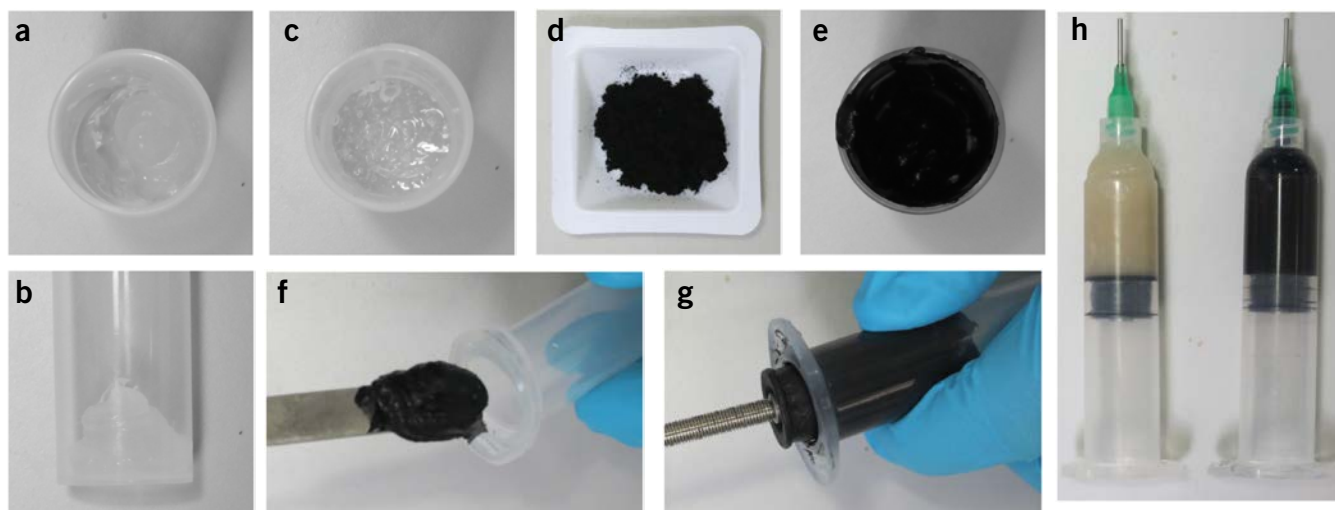


Figure 8 | Preparation of acetoxy-silicone composite catalyst 'inks' for printing catalyst beds. The full process is shown for the Pd/C composite material; however, the individual steps are identical for the preparation of both catalyst materials. (a,b) Approximately 4.2 g of LOCTITE 5366 sealant in a 25-ml-capacity disposable PP sample container. (c) Step 17: acetoxy-silicone after thinning with 2.0 ml of toluene. It is necessary to thin the acetoxy-silicone in this way before the addition of the catalyst material to ensure the correct viscosity of the resulting material for printing. (d) Step 18: 0.5 g of 10% Pd/C catalyst. (e) Step 18: composite material after mixing the catalyst powder with the thinned acetoxy-silicone. (f) Step 19: transfer of composite catalyst material into 10-ml-capacity PP dispensing syringe suitable for use with Fab@Home 3D printer. (g) Step 20: fitting the Fab@Home plunger into the dispensing syringe. (h) Step 20: the filled syringes with montmorillonite K10 (left) and Pd/C (right) composite catalyst materials ready for installation into the Fab@Home printer.

obtained (**Fig. 8e**). This loading of material into the print matrix is sufficient to produce a material with the desired viscosity to print in a manner similar to pure silicone polymer.

19| By using a spatula, transfer the resulting material into a receptacle for printing in the soft material 3D printer. For the Fab@Home device used by the authors, this is a 10-ml-capacity dispensing syringe barrel fitted with a 0.838-mm internal diameter dispensing tip (**Fig. 8f**).

▲ **CRITICAL STEP** It is important to avoid introducing air bubbles into the material at this stage, as any voids present in the syringe will lead to uneven printing of the material.

20| Fit the FAB@Home syringe plunger into the barrel (**Fig. 8g**) and fit the syringe (**Fig. 8h**) into the Fab@Home printer.

21| Upload the .stl files relevant to the parts to be printed using the composite materials or acetoxy-silicone polymer (see Step 1). Use the printer control software to assign the correct material settings and syringe positions. The Fab@Home printer used by the authors allows two material syringes to be fitted and printed with simultaneously, and the control software allows more materials to be chosen, which can be fitted during the printing process; there are a number of preset material setting profiles, of which the acetoxy-silicone polymer is one. It is possible for the user to create bespoke material profiles using the Fab@Home printer by adjusting the print settings; for further information, see the **Supplementary Discussion**.

Composite material printing ● TIMING 48 h

22| Once the PP printer has paused at the preset pause point, ensure that the print head has moved to the rest position and that it has cooled to a safe level (**Fig. 9a**).

23| Remove the PP print bed from the printer and transfer it to the second (soft material) printer.

▲ **CRITICAL STEP** The print bed must be affixed to the secondary printer's print surface similarly to the first printer, by making sure to align the print bed carefully with the printer's origin point, which was determined in Step 8 (**Fig. 9b**).

24| Begin the printing process on the soft material printer and observe the progress.

25| Once a maximum of three layers of material have been deposited, pause the print process and, if further layers are required, transfer the print bed back to the PP printer to allow further printing of the structure.

26| Repeat the transfer process (Steps 22–25) as many times as necessary to complete the desired design. In the example case, only one pause is required for the printing of the 10% Pd/C and the montmorillonite K10-doped acetoxy-silicone beds in chambers 1 and 3 of the reactor (**Fig. 9c**).

27| After the last phase of soft material printing, allow the print to stand at room temperature (20 °C) and in an extracting fume hood for 24 h to allow for curing of the acetoxy-silicone matrix (and the removal of the acetic acid produced during this process) and to allow for the evaporation of most of the toluene used for thinning. It is normal to observe some shrinkage in the resulting structures at this stage. After 24 h, the print bed should be washed three times with deionized water and subsequently placed in an extracting fume hood and allowed to dry for an additional 18 h (overnight). As the

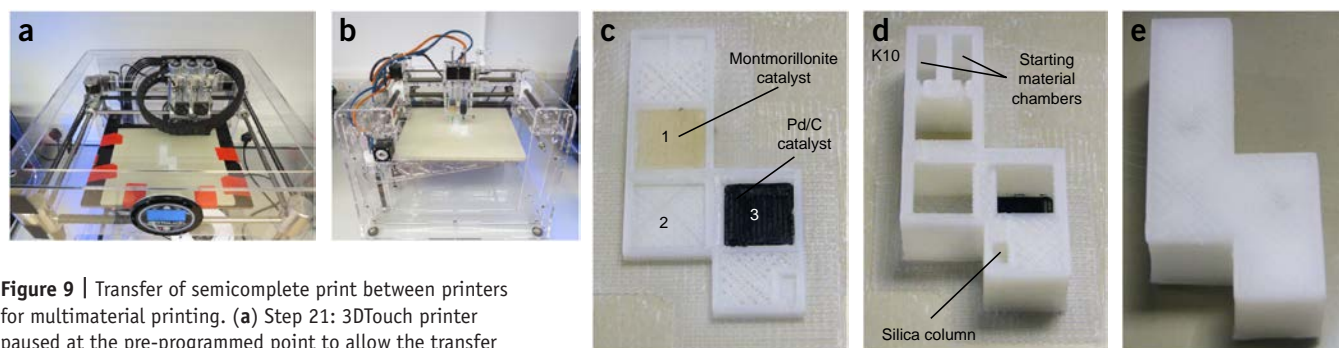


Figure 9 | Transfer of semicomplete print between printers for multimaterial printing. **(a)** Step 21: 3DTouch printer paused at the pre-programmed point to allow the transfer of the print bed to the Fab@Home printer for printing of the catalyst beds into the structure. **(b)** Step 22: the print bed is affixed to the Fab@Home printer, with care taken to align it correctly with the printer's center point. **(c)** Reactionware architecture after printing of catalyst beds before transfer back to 3DTouch for continued PP printing. **(d)** Second pause in the PP printing: the device is ready for the introduction of the purification column and the starting materials and reagents necessary for the reactionware experiment. **(e)** Completed reactionware device ready for use.

PROTOCOL

reactionware device is sealed, curing and washing of the device must be carried out when the acetoxy-silicone parts are still exposed before continuing to print the PP architecture. If this is not the case and the design is such that it leaves the soft material parts sufficiently exposed to allow for curing and washing of the completed device, this stage can be carried out after the completion of reactionware printing.

Printing of further PP architecture ● TIMING variable

28| Return the print bed to the PP printer (3DTouch), making sure to align the print bed carefully as described in Step 8.

29| Restart the PP printing and observe the process for two to three layers to ensure that the model is correctly aligned and the new layers are adhering adequately to the already printed part.

Insertion of nonprinted components ● TIMING 20–25 min

30| Once the PP printer has paused at the preset pause point, ensure that the print head has moved to the rest position and cooled to a safe level. It is then safe to insert the nonprinted parts into the correct position in the part-printed object.

31| Place a small quantity of glass wool in the bottom of the purification column cavity (**Fig. 9d**), and pack it tightly using a glass stirring rod. Insert a second small piece of glass wool into the channel between the cavity and the final reaction chamber.

32| Deposit 0.1 g of Celite 535 into the same cavity, and once again pack tightly with a glass stirring rod.

33| Suspend 1 g of silica gel in *n*-hexane to form a slurry. By using a wide-bore Pasteur pipette (the authors use 3-ml-capacity disposable PP Pasteur pipettes), transfer enough of this slurry into the cavity to fill it with liquid. Allow this to settle for 2–3 min, and pipette off the *n*-hexane from the top of the cavity; refill the space with fresh silica slurry. Repeat this process until the cavity is filled with silica. Tamp the silica into the cavity with a glass stirring rod, and repeat the process until no further silica can be added.

! CAUTION Organic solvents such as *n*-hexane should be handled using appropriate protective equipment such as nitrile gloves and lab coats and should generally be used in an extracting fume hood.

34| Place a 1.5 × 5 mm Teflon-coated magnetic stirring bar into each of the three reaction chambers.

35| Deposit solutions of acrolein (1 mmol, 56 mg, 47 μl) and 1,2,3,4,5-pentamethylcyclopentadiene (1 mmol, 136 mg, 118 μl) in 5% diethyl ether/hexane (0.750 ml each) into the starting material chambers of the part-printed device and a solution of aniline (1 mmol) in a mixture of triethylsilane (10 mmol) and MeOH (0.2 ml) into the second reaction chamber.

Finishing PP printing ● TIMING variable

36| Return the print bed to the final printer to finish the fabrication of the reactionware device (**Fig. 9e**).

37| Once the printing process is finished and the print head has returned to the home position and cooled sufficiently, remove the print bed from the printer and use a large flat blade (the authors use a blade initially designed for wallpaper removal) to detach the print from the print bed.

38| Inspect the device for obvious flaws in printing, such as poor layer adhesion, which may necessitate the reprinting of the device.

39| If the device appears well printed, it is now ready for testing under the desired circumstances of the experiment, and any postprinting modification of the device can now be carried out.

? TROUBLESHOOTING

Troubleshooting advice can be found in **Table 1**.

The following table gives a reference to the most common errors associated with printing reactionware in PP by an FDM method. This should be considered in conjunction with the **Supplementary Discussion** on PP print settings, as most common errors are associated with incorrect or suboptimal print settings; these errors are most likely to occur during Steps 12–15, 28 and 36–39. Further, printer-specific troubleshooting advice can generally be found on the internet at 3D printer manufacturers' websites (some examples are RepRap-based printers (http://reprap.org/wiki/Print_Troubleshooting_Pictorial_Guide) and Ultimaker (<https://ultimaker.com/en/support/visual-troubleshooting-guide>)).

TABLE 1 | Troubleshooting table.

Step	Problem	Possible reason	Solution
4	Print is delaminating	Step size along z-axis is too large ('layer height')	Decrease the layer thickness in the material settings and prepare the print instruction file again
		Extrusion temperature too low	Increase the temperature of the hot-end during print (try +5–10 K)
	Small voids close up	Over extrusion	Decrease the flow rate (or the flow multiplier) in the print settings
	Inner dimensions in general are smaller than designed	Wrong filament diameter selected in the slicing software	Select the correct filament diameter (typically 1.75, 2.85 or 3 mm)
	Outer boundaries look very 'layered'	Wrong nozzle size in the slicing software	Pick the correct nozzle size
	Solid layers not closed completely	Underextrusion	Increase the flow multiplier in the printer configuration
	Filament getting stuck completely		Use a different hot-end or polymer at the SETUP stage
	Gaps in the extruded filament	Wrong nozzle size in the slicing software	Pick the correct nozzle size
		Wrong filament diameter selected in the slicing software	Select the correct filament diameter (typically 1.75, 2.85 or 3 mm)
		Extruder temperature too low	Increase the extrusion temperature when the filament does not get pushed through the nozzle at the intended speed
5	Printed reactionware leaks	Underextrusion	As above
		Wrong infill structure	Pick a different, more dense infill structure or just increase the density of the one currently in use
8	Print is detaching from the print bed	Not enough solid layers before infill	Increase the number of solid layers in the slicing software
		The surface or material of the bed is wrong for the polymer used to print	Try coating the print bed with glue from a glue stick or covering it with masking tape to increase mechanical adhesion of the polymer to the bed Try different bed types (carbon fiber, glass and so on, depending on the printing material)
9		z-Height home too far off the bed	Ensure that the nozzle of the extruder is about 100–200 μm off the bed in all places when homed. If not, re-align it
15			Check that the feed wheel of the extrusion mechanism has not 'eaten' into the filament and hence does not push it forward anymore Alternatively, the pressure on the filament could be too low to ensure correct movement (check whether the filament actually moves as intended)

PROTOCOL

TIMING

- Steps 1–6, preparation of the print file: variable
- Steps 7–11, preparation of PP 3D printer: 20 min
- Steps 12–15, printing the PP architecture: variable depending on the design; it generally takes several hours
- Steps 16–19, preparation of composite catalyst materials for printing: 10–15 min
- Steps 20–26, printing of composite catalyst materials: no more than 3–4 h
- Step 27, curing and washing catalyst materials: at least 42 h
- Steps 28 and 29, further printing of PP architecture: variable
- Steps 30–35, insertion of nonprinted components: 20–25 min
- Steps 36–39, finishing PP printing: variable

ANTICIPATED RESULTS

The anticipated results for the general printing of reactionware will depend on the exact purpose to which the device is put, along with the specific experiment being carried out. For a full discussion of the development and concept behind the above protocol, see our previously published research paper covering the work²⁰. Once the reactionware produced from this procedure is complete, it should be removed from the PP print bed, and the process of conducting the synthetic reaction is initiated by tilting the device by 45° to transfer the starting materials into the first reaction chamber. The device is then manipulated through a series of 90° rotations that are designed to transfer the reaction mixture through the sequential reaction chambers (Fig. 10a). The reaction is allowed to rest in each chamber for sufficient time to complete each reaction stage, and the product is retrieved by piercing a needle through the sealed opening at the bottom of the purification column and slowly drawing out the reaction mixture through the purification column, yielding a mixture of endostructural and exostructural isomers of 1,4,5,6,7-pentamethyl-bicyclo(2.2.1)hept-2-ylmethyl-phenyl-amine, C₁₉H₂₉N. Factors that may affect this result include failure of the printing process, such as poor alignment of the print bed upon transferring the print between 3D printers (Fig. 10b), or insufficient packing of the silica column (Step 31), leading to impurities being present in the final product (Fig. 10c). Unfortunately, because of the monolithic nature of the reactionware printed using this protocol, these failures generally require reprinting of the reactionware. If the print and reaction are successful, a relatively clean ¹H NMR spectrum should be obtained from the resulting material after removal of excess solvent under reduced pressure (Fig. 10d).

(1,4,5,6,7-Pentamethyl-bicyclo(2.2.1)hept-2-ylmethyl)-phenyl-amine (3): pale yellow oil

¹H NMR (400 MHz, CDCl₃) δ (major product) δ 7.10–7.06 (m, 2H), 6.59 (tt, 1H, J₁=7.3, J₂=1.0 Hz), 6.48 (dt, 2H, J₁=8.6, J₂=1.0 Hz), 3.4 (broad s, 1H), 3.05 (dd, 1H, J₁=11.0, J₂=4.6 Hz), 2.38–2.34 (m, 1H), 1.99–1.94 (m, 1H), 1.63–1.58 (m, 1H), 1.56–1.51 (m, 1H), 1.48 (d, 3H, J=1.0 Hz), 1.44 (d, 3H, J=1.2 Hz), 1.43–1.40 (m, 1H), 1.24 (q, 1H, J=6.4 Hz) 1.05 (s, 3H), 0.98–0.93 (m, 1H), 0.94 (s, 3H), 0.50 (d, 3H, J=6.4 Hz). (Minor product) δ 7.11–7.08 (m, 2H), 6.60 (dt, 1H, J₁=7.3, J₂=1.1 Hz), 6.52 (dt, 2H, J₁=8.6, J₂=1.1 Hz), 3.20 (dd, 1H, J₁=11.3, J₂=5.0 Hz), 3.01 (dd, 1H, J₁=11.1, J₂=4.1), 2.83–2.78 (m, 1H), 2.41–2.36 (m, 1H), 1.77–1.73 (m, 1H), 1.48–1.47 (m, 3H), 1.43–1.44 (m, 3H), 1.39–1.37 (m, 1H), 1.21–1.18 (m, 1H), 1.06 (s, 3H), 0.96 (s, 3H), 0.68–0.64 (m, 1H), 0.52 (d, 3H, J=4.5).

¹³C NMR (125 MHz, CDCl₃) δ (major product) δ 7.8 (CH₃), 9.6 (CH₃), 9.7 (CH), 12.2 (CH₃), 14.8 (CH), 14.3 (CH₃), 15.4 (CH₃), 40.6 (CH₂), 47.1 (CH₂), 48.6 (CH), 52.5 (C_q), 55.9 (C_q), 61.8 (CH), 112.7 (CH-Ar), 117.0 (CH-Ar), 129.1 (CH-Ar), 134.9 (C_q-Ar). (Minor product) δ 8.0 (CH₃), 9.3 (CH₃), 9.4 (CH), 12.04 (CH), 12.8 (CH₃), 13.8 (CH₃), 15.3 (CH₃), 42.1 (CH₂), 45.6 (CH), 47.6 (CH₂), 52.6 (C_q), 55.2 (C_q), 61.7 (CH), 112.8 (CH-Ar), 117.1 (CH-Ar), 129.1 (CH-Ar), 135.3 (C_q-Ar).

HRMS (MH⁺) calcd. (found) for C₁₉H₂₉N: 272.2373 (272.2399).

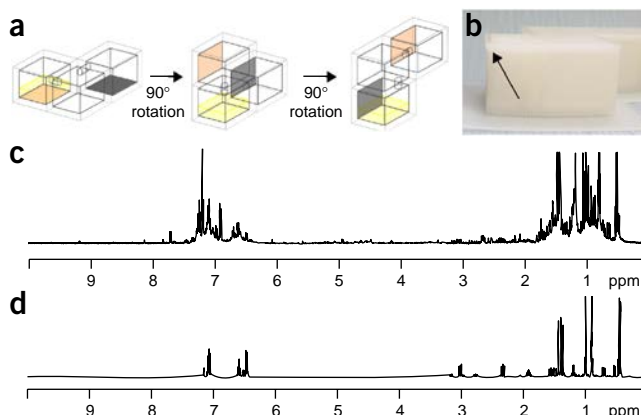


Figure 10 | Function of the completed reactionware device and anticipated results. (a) Schematic diagram of the rotation sequence of the example reactionware required to synthesize the desired product, 1,4,5,6,7-pentamethyl-bicyclo(2.2.1)hept-2-ylmethyl-phenyl-amine, C₁₉H₂₉N. (b) Example of poor alignment (indicated by arrow) of the print bed upon returning the reactionware to the PP 3D printer after insertion of the nonprinted parts leading to a flaw in the printing. This device was invalid for use in the experiment, as the misalignment caused the device to leak when rotated. (c) Example ¹H NMR spectrum of a poorly purified reaction mixture caused by insufficient packing of silica material during the reactionware fabrication. (d) Example of a ¹H NMR spectrum resulting from a successful completion of the reactionware experiment.

Note: Any Supplementary Information and Source Data files are available in the online version of the paper.

ACKNOWLEDGMENTS We gratefully acknowledge financial support from the EPSRC (grants EP/L023652/1, EP/K038885/1, EP/H024107/1, EP/K023004/1, EP/K021966/1, EP/I033459/1, EP/J015156/1, EVOLISS EC 611640, EVOPROG EC 610730 and MICREAGENTS EC 318671 to L.C.), the Fundamental Research Funds for the Central Universities project (grants buctrc201510 and buctrc201530 to Y.-F.S. and L.C.) and the Royal Society Wolfson Foundation for a Merit Award. We acknowledge the work of M.D. Symes, R.S. Forgan, V. Sans, M.H. Rosnes and V. Dragone for their contributions to the development of the applications of this protocol.

AUTHOR CONTRIBUTIONS P.J.K. designed and performed the experiments, analyzed data and wrote the paper with guidance from L.C.; S.G. contributed extensively to the editing of the paper and with expertise in 3D printing theory and practice; W.C. and C.-G.L., supervised by Y.-F.S., contributed to the generalization of the protocol; L.C. conceived the idea, supervised the project and designed the experiments.

COMPETING FINANCIAL INTERESTS The authors declare competing financial interests: details are available in the online version of the paper.

Reprints and permissions information is available online at <http://www.nature.com/reprints/index.html>.

1. Dimitrov, D., Schreive, K. & de Beer, N. Advances in three dimensional printing – state of the art and future perspectives. *Rapid Prototyping J.* **12**, 136–147 (2006).
2. Gibson, I., Rosen, D. & Stucker, B. *Additive Manufacturing Technologies* 2nd edn. (Springer-Verlag, 2015).
3. Rengier, F. *et al.* 3D printing based on imaging data: review of medical applications. *Int. J. Comput. Assist. Radiol. Surg.* **5**, 335–341 (2010).
4. Li, X.M. *et al.* 3D-printed biopolymers for tissue engineering application. *Int. J. Polym. Sci.* **2014**, 1–13 (2014).
5. Skoog, S.A., Goering, P.L. & Narayan, R.J. Stereolithography in tissue engineering. *J. Mater. Sci. Mater. Med.* **25**, 845–856 (2014).
6. Hollister, S.J. Porous scaffold design for tissue engineering. *Nat. Mater.* **4**, 518–524 (2005).
7. Barry, R.A. *et al.* Direct-write assembly of 3D hydrogel scaffolds for guided cell growth. *Adv. Mater.* **21**, 2407–2410 (2009).
8. Hong, S. *et al.* 3D printing of highly stretchable and tough hydrogels into complex, cellularized structures. *Adv. Mater.* **27**, 4035–4040 (2015).
9. Nakamura, M. *et al.* Biomatrices and biomaterials for future developments of bioprinting and biofabrication. *Biofabrication* **2**, 014110 (2010).
10. Boland, T., Xu, T., Damon, B. & Cui, X. Application of inkjet printing to tissue engineering. *Biotechnol. J.* **1**, 910–917 (2006).
11. Zhang, Y., Tse, C., Rouholamin, D. & Smith, P. Scaffolds for tissue engineering produced by inkjet printing. *Cent. Eur. J. Eng.* **2**, 325–335 (2012).
12. Mohanty, S. *et al.* Fabrication of scalable and structured tissue engineering scaffolds using water dissolvable sacrificial 3D printed moulds. *Mater. Sci. Eng. C* **55**, 569–578 (2015).
13. Kolesky, D.B. *et al.* 3D bioprinting of vascularized, heterogeneous cell-laden tissue constructs. *Adv. Mater.* **26**, 3124–3130 (2014).
14. Mosadegh, B., Xiong, G., Dunham, S. & Min, J.K. Current progress in 3D printing for cardiovascular tissue engineering. *Biomed. Mater.* **10**, 034002 (2015).
15. Habibovic, P. *et al.* Osteoconduction and osteoinduction of low-temperature 3D printed bioceramic implants. *Biomaterials* **29**, 944–953 (2008).
16. Klammert, U. *et al.* Low temperature fabrication of magnesium phosphate cement scaffolds by 3D powder printing. *J. Mater. Sci. Mater. Med.* **21**, 2947–2953 (2010).
17. Ley, S.V., Fitzpatrick, D.E., Ingham, R.J. & Myers, R.M. Organic synthesis: march of the machines. *Angew. Chem. Int. Ed.* **54**, 3449–3464 (2015).
18. Gross, B.C., Erkal, J.L., Lockwood, S.Y., Chen, C. & Spence, D.M. Evaluation of 3D printing and its potential impact on biotechnology and the chemical sciences. *Anal. Chem.* **86**, 3240–3253 (2014).
19. Symes, M.D. *et al.* Integrated 3D-printed reactionware for chemical synthesis and analysis. *Nat. Chem* **4**, 349–354 (2012).

20. Kitson, P.J., Symes, M.D., Dragone, V. & Cronin, L. Combining 3D printing and liquid handling to produce user-friendly reactionware for chemical synthesis and purification. *Chem. Sci.* **4**, 3099–3103 (2013).
21. Jakus, A.E. *et al.* Three-dimensional printing of high-content graphene scaffolds for electronic and biomedical applications. *ACS Nano* **9**, 4636–4648 (2015).
22. Lewis, J.A. Direct ink writing of 3D functional materials. *Adv. Funct. Mater.* **16**, 2193–2204 (2006).
23. Kong, Y.L. *et al.* 3D printed quantum dot light-emitting diodes. *Nano Lett.* **14**, 7017–7023 (2014).
24. Austin-Morgan, T. 3D printing of optical fibre. *New Electron.* **48**, 8 (2015).
25. Pham, D.T. & Gault, R.S. A comparison of rapid prototyping technologies. *Int. J. Mach. Tools Manuf.* **38**, 1257–1287 (1998).
26. Wang, X. *et al.* i3DP, a robust 3D printing approach enabling genetic post-printing surface modification. *Chem. Commun.* **49**, 10064–10066 (2013).
27. Xing, J.-F., Zheng, M.-L. & Duan, X.-M. Two-photon polymerization microfabrication of hydrogels: an advanced 3D printing technology for tissue engineering and drug delivery. *Chem. Soc. Rev.* **44**, 5031–5039 (2015).
28. Tumbleston, J.R. *et al.* Continuous liquid interface production of 3D objects. *Science* **347**, 1349–1352 (2015).
29. Park, S.H., Yang, D.Y. & Lee, K.S. Two-photon stereolithography for realizing ultraprecise three-dimensional nano/microdevices. *Laser Photon. Rev.* **3**, 1–11 (2009).
30. Wallace, D. in Inkjet-based Micromanufacturing Vol. 9 *Advanced Micro and Nanosystems* (eds. Korvink, J.G., Smith, P.J. & Shin, D.-Y.) 1–14 (Wiley-VCH, 2012).
31. Shirazi, S.F.S. *et al.* A review on powder-based additive manufacturing for tissue engineering: selective laser sintering and inkjet 3D printing. *Sci. Technol. Adv. Mater.* **16**, 20 (2015).
32. Lee, K. *et al.* 3D-printed alginate/phenamil composite scaffolds constituted with micro-sized core-shell struts for hard tissue regeneration. *RSC Adv.* **5**, 29335–29345 (2015).
33. Mironov, V., Boland, T., Trusk, T., Forgacs, G. & Markwald, R.R. Organ printing: computer-aided jet-based 3D tissue engineering. *Trends Biotechnol.* **21**, 157–161 (2003).
34. Dorey, E. Process technology 3D printing for drugs. *Chem. Ind.* **78**, 7 (2014).
35. Icten, E., Giridhar, A., Taylor, L.S., Nagy, Z.K. & Reklaitis, G.V. Dropwise additive manufacturing of pharmaceutical products for melt-based dosage forms. *J. Pharm. Sci.* **104**, 1641–1649 (2015).
36. Kumar, S. Selective laser sintering: a qualitative and objective approach. *JOM J. Miner. Met. Mater. Soc.* **55**, 43–47 (2003).
37. Agarwala, M., Bourell, D., Beaman, J., Marcus, H. & Barlow, J. Direct selective laser sintering of metals. *Rapid Prototyping J.* **1**, 26–36 (1995).
38. Fischer, P. *et al.* Sintering of commercially pure titanium powder with a Nd: YAG laser source. *Acta Mater.* **51**, 1651–1662 (2003).
39. Wang, F.L., Yi, C.Y., Wang, T., Yang, S.Z. & Zhao, G. A generating method for digital gear tooth surfaces. *Int. J. Adv. Manuf. Technol.* **28**, 474–485 (2006).
40. Capel, A.J. *et al.* Design and additive manufacture for flow chemistry. *Lab Chip* **13**, 4583–4590 (2013).
41. Hwang, Y.H., Paydar, O.H. & Candler, R.N. 3D printed molds for non-planar PDMS microfluidic channels. *Sens. Actuat. A Phys.* **226**, 137–142 (2015).
42. Mathieson, J.S., Rosnes, M.H., Sans, V., Kitson, P.J. & Cronin, L. Continuous parallel ESI-MS analysis of reactions carried out in a bespoke 3D printed device. *Beilstein J. Nanotechnol.* **4**, 285–291 (2013).
43. Dragone, V., Sans, V., Rosnes, M.H., Kitson, P.J. & Cronin, L. 3D-printed devices for continuous-flow organic chemistry. *Beilstein J. Org. Chem.* **9**, 951–959 (2013).
44. Kitson, P.J., Rosnes, M.H., Sans, V., Dragone, V. & Cronin, L. Configurable 3D-printed millifluidic and microfluidic ‘lab on a chip’ reactionware devices. *Lab Chip* **12**, 3267–3271 (2012).
45. Lee, M.P. *et al.* Development of a 3D printer using scanning projection stereolithography. *Sci. Rep.* **5**, 9875 (2015).
46. Campbell, T.A. & Ivanova, O.S. 3D printing of multifunctional nanocomposites. *Nano Today* **8**, 119–120 (2013).
47. Guo, S.-Z., Yang, X., Heuzey, M.-C. & Therrault, D. 3D printing of a multifunctional nanocomposite helical liquid sensor. *Nanoscale* **7**, 6451–6456 (2015).
48. Kim, J.H. *et al.* 3D printing of reduced graphene oxide nanowires. *Adv. Mater.* **27**, 157–161 (2015).



49. Peterson, G.I., Larsen, M.B., Ganter, M.A., Storti, D.W. & Boydston, A.J. 3D-printed mechanochromic materials. *ACS Appl. Mater. Interfaces* **7**, 577–583 (2015).
50. Postiglione, G., Natale, G., Griffini, G., Levi, M. & Turri, S. Conductive 3D microstructures by direct 3D printing of polymer/carbon nanotube nanocomposites via liquid deposition modeling. *Compos. A Appl. Sci. Manuf.* **76**, 110–114 (2015).
51. Visser, C.W. *et al.* Toward 3D printing of pure metals by laser-induced forward transfer. *Adv. Mater.* **27**, 4087–4092 (2015).
52. Wei, X. *et al.* 3D printable graphene composite. *Sci. Rep.* **5**, 11181 (2015).
53. Malone, E. *et al.* Freeform fabrication of zinc-air batteries and electromechanical assemblies. *Rapid Prototyping J.* **10**, 58–69 (2004).
54. Ferrari, S. *et al.* Latest advances in the manufacturing of 3D rechargeable lithium microbatteries. *J. Power Sources* **286**, 25–46 (2015).
55. Trimmer, B., Lewis, J.A., Shepherd, R.F. & Lipson, H. 3D printing soft materials: what is possible? *Soft Robot.* **2**, 3–6 (2015).
56. Ilievski, F., Mazzeo, A.D., Shepherd, R.F., Chen, X. & Whitesides, G.M. Soft robotics for chemists. *Angew. Chem. Int. Ed.* **50**, 1890–1895 (2011).
57. Melin, J. & Quake, S.R. in Annual Review of Biophysics and Biomolecular Structure. Vol. 36 *Annual Review of Biophysics* 213–231 (Annual Reviews, 2007).
58. Kitson, P.J., Marshall, R.J., Long, D., Forgan, R.S. & Cronin, L. 3D printed high-throughput hydrothermal reactionware for discovery, optimization, and scale-up. *Angew. Chem. Int. Ed.* **53**, 12723–12728 (2014).
59. Loiseau, T. *et al.* MIL-96, a porous aluminum trimesate 3D structure constructed from a hexagonal network of 18-membered rings and μ 3-oxo-centered trinuclear units. *J. Am. Chem. Soc.* **128**, 10223–10230 (2006).